Sound absorption theory for micro-perforated panel with petal-shaped perforations

Zhimin Xu, Wei He, Xiangjun Peng, Fengxian Xin, and Tian Jian Lu

Citation: The Journal of the Acoustical Society of America **148**, 18 (2020); doi: 10.1121/10.0001462
View online: https://doi.org/10.1121/10.0001462
View Table of Contents: https://asa.scitation.org/toc/jas/148/1
Published by the Acoustical Society of America

JASA ARTICLE

Sound absorption theory for micro-perforated panel with petal-shaped perforations

Zhimin Xu,[1] Wei He,[1] Xiangjun Peng,[1] Fengxian Xin,[1,a)] and Tian Jian Lu[2,b)]

[1]*State Key Laboratory for Strength and Vibration of Mechanical Structures, Xi'an Jiaotong University, Xi'an 710049, People's Republic of China*

[2]*State Key Laboratory of Mechanics and Control of Mechanical Structures, Nanjing University of Aeronautics and Astronautics, Nanjing 210016, People's Republic of China*

ABSTRACT:

Micro-perforated panel (MPP) absorbers with circular perforations are used in many noise control applications due to their attractive wide-brand sound absorption performance. Different from a common MPP with circular perforations, a unique type of MPP absorber with petal-shaped perforations is proposed. The sound absorption theory for the MPP with petal-shaped perforations is developed by accurately considering the fluid velocity in the petal-shaped perforation hole. This theory can account for the effect of altered perforation morphology (from circular to petal) on sound absorption. Finite element simulations are performed to validate the proposed theory, with good agreement achieved. The sound absorption of MPP with petal-shaped perforations is compared with that of the traditional MPP with the same porosity. It is demonstrated that the change in hole shape significantly modifies the fluid velocity field and the flow resistivity in/of the hole, and hence the sound absorption of the proposed MPP with petal-shaped perforations can outperform that of the traditional MPP in the considered case. This work proposes a general MPP theory that not only contains the classical Maa's theory for circular MPP, but also accounts for the MPP with petal-shaped perforations. © *2020 Acoustical Society of America*. https://doi.org/10.1121/10.0001462

(Received 5 March 2020; revised 1 June 2020; accepted 5 June 2020; published online 1 July 2020)

[Editor: Ning Xiang] Pages: 18–24

To inhibit noise pollution, numerous sound absorbing materials and structures have been developed. Traditional sound absorbing materials, such as open-celled foams and fibrous wool, deteriorate over time as small particles are often dislodged from the skeleton of these porous materials.[1] Further, the dislodged small particles may contaminate the air inside buildings and endanger human health. As a result, perforated panel absorbers are attractive choice for buildings and dwelling houses. As a resonant structure, the perforated panel absorber is composed of two parts: a thin panel with periodical perforations and a backing cavity. The perforations, with diameters in the scale of millimeter or even centimeter, typically have relatively small acoustic resistance, thus requiring inserting porous materials into the backing cavity for enhanced sound absorption. The use of porous materials sets a considerable limit on the application of perforated panel absorbers. To address this deficiency, Maa[2,3] put forward the concept of a micro-perforated panel (MPP) and developed a sound absorption theory for the MPPs. Different from the perforated panel absorbers, the MPPs have sub-millimeter hole sizes and hence sufficient acoustic resistance and low acoustic mass reactance, enabling wide-band sound absorption without the use of additional porous material inside the backing cavity.

As is well-known, the MPP with a backed cavity is a typical Helmholtz resonator. The loss of sound energy depends mainly on the viscous dissipation of air oscillating in the perforations. Thus, it is expected that the morphology of the perforation could greatly affect the sound absorption performance of MPPs. To achieve superior acoustic performance, different approaches have been attempted to tailor the design of micro-perforations. One approach is to bend the perforation to form a curved axial or roughened perforation so that its effective path becomes elongated.[4–6] Another method introduces surface roughness to the perforation along the propagation path of sound, so as to increase the air flow resistivity (thus the sound absorption).[7]

In the current study, the cross-sectional morphology of the traditionally circular perforations is systematically varied and a general MPP theory is proposed to account for the effect of perforation shape on sound absorption. It is anticipated that changing the perforation shape from circle to petal enlarges the surface impedance of the MPP and hence its absorption performance can be enhanced in certain cases. Guo *et al*. proposed a model to calculate the sound absorption of a MPP with non-circular perforations,[8] which uses the hydraulic radius of the non-circular perforations to approximately represent the influence of perforation shape. In the current study, a different approach is adopted. First, by regarding the petal-shaped perforation as a circular hole

[a)]Also at: MOE Key Laboratory for Multifunctional Materials and Structures, Xi'an Jiaotong University, Xi'an 710049, People's Republic of China. Electronic mail: fengxian.xin@gmail.com, ORCID: 0000-0001-8855-5366.

[b)]Also at: Nanjing Center for Multifunctional Lightweight Materials and Structures (MLMS), Nanjing University of Aeronautics and Astronautics, Nanjing 210016, People's Republic of China.

https://doi.org/10.1121/10.0001462

with sinusoidal disturbance, a theoretical solution for fully developed laminar flow in idealized petal-shaped holes is obtained in a previous study using the perturbation method,[9] with the petal-shaped hole assumed infinitely long along its axial direction. This solution is used to determine the influence of the non-circular perforation shape on static flow resistivity and tortuosity of the perforation, which are used to calculate the acoustic impedance. From this point of view, for MPPs with non-circular perforations, the model of Guo *et al* is simpler but approximate, while the present model is more accurate.

As shown in Fig. 1(a), a plane sound wave incidents perpendicularly on a MPP with periodically arranged, petal-shaped micro-perforations. Due to periodicity, only one micro-perforation needs to be considered. Let t denote the thickness of the panel and D the thickness of the backing cavity. Figure 1(b) depicts the details of a petal-shaped perforation, where d is the average diameter and $2e$ is the magnitude of radial fluctuation of the petal-shaped micro-perforation relative to a circular micro-perforation of diameter d. Mathematically, the profile of the petal-shaped micro-perforation can be expressed in a cylindrical coordinate system [Fig. 1(b)] as

$$\rho = d[0.5 - \varepsilon \sin(n\theta)], \tag{1}$$

in which $\varepsilon = e/d$ is defined here as the relative roughness to quantify the relative fluctuation amplitude of the perforation profile and n is the number of sinusoidal waves in the petal-shaped perforation morphology [e.g., $n = 8$ in Fig. 1(b)].

Sound absorption of the MPP system is mainly contributed by viscous dissipation through friction within the boundary layers inside the micro-perforations; dissipation of sound energy via heat loss route is in general negligible. By electro-acoustic analogy, the specific sound absorption coefficient of the MPP can be calculated once its acoustical resistance and acoustical reactance are determined.

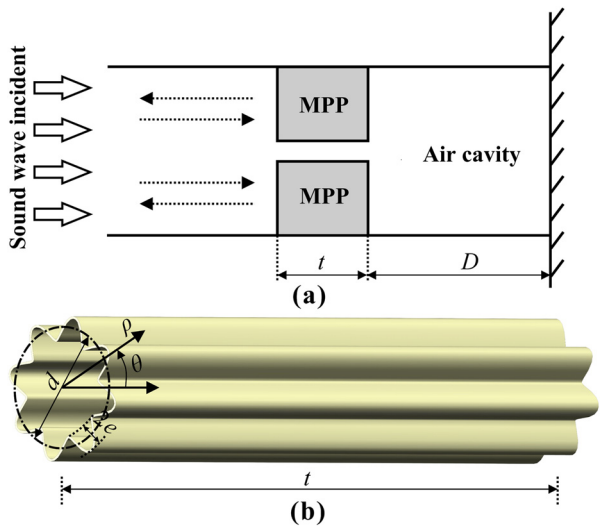

FIG. 1. (Color online) Schematic of sound wave incident on a MPP with petal-shaped perforations.

Following Maa's[2,3] theory, the sound absorption coefficient of the MPP can be expressed as

$$\alpha = \frac{4r}{(1+r)^2 + [\omega m - \cot(\omega D/c)]^2}, \tag{2}$$

where r is the relative acoustic resistance, m is the relative acoustic mass, ω is the angular frequency of incident acoustic wave, D is the thickness of cavity as shown in Fig. 1(a), and c is the sound speed in air ($c = 340$ m/s in the current study). Since the MPP sound absorption system is essentially a Helmholtz resonator, there exists a frequency, ω_0, at which the air inside the hole approaches to the resonant condition, leading to a sound absorption peak. From Eq. (2), the sound absorption coefficient reaches its maximum value,

$$\alpha_m = \frac{4r}{(1+r)^2} \tag{3}$$

at frequency ω_0, which satisfies

$$\omega_0 m = \cot(\omega_0 D/c). \tag{4}$$

To determine r and m, the acoustic impedance z of the MPP needs to be calculated. For circular perforations, applying the classical Maa's theory leads to

$$\begin{aligned} z &= r + \mathrm{j}\omega m \\ &= \frac{\mathrm{j}\omega t}{\phi c}\left[1 - \frac{2}{k\sqrt{-\mathrm{j}}}\frac{J_1(k\sqrt{-\mathrm{j}})}{J_0(k\sqrt{-\mathrm{j}})}\right]^{-1} + \frac{4\sqrt{2}\mu k}{\phi \rho_0 c d} \\ &\quad + \mathrm{j}\frac{0.85\omega d}{\phi c}, \end{aligned} \tag{5}$$

where $\mathrm{j} = \sqrt{-1}$ is the imaginary unit, $k = d\sqrt{\rho\omega/4\mu}$ is the ratio of hole size to the thickness of viscous boundary layer, d is the hole diameter, ρ_0 is the density of air, μ is the dynamic viscosity of air, ϕ is the porosity of the MPP, J_1 is the Bessel function of the first kind and first order, and J_0 is the Bessel function of the first kind and zeroth order. The first term of Eq. (5) represents the viscous effect inside the holes, while the last two terms reflect the end effects corresponding to sound dissipation and sound radiation around the inlet and outlet of the MPP, respectively. For a traditional MPP with circular perforations, the sound absorption coefficient is calculated by inserting the above (r, m) into Eq. (2).

For the proposed MPP with petal-shaped holes, in order to calculate its acoustic impedance, the flow field of air in the petal-shaped perforation hole needs to be determined first. By regarding the petal-shaped perforation as a circular hole with sinusoidal disturbance, a theoretical solution for fully developed laminar flow in idealized petal-shaped holes was obtained in a previous study using the perturbation method,[9] with the petal-shaped hole assumed infinitely long along its axial direction. The axial velocity of air can then be explicitly expressed in the cylindrical coordinate system of Fig. 1(b) as

$$u = \left[2 - 2(1-2\varepsilon)^{-2} + \left(8(1-2\varepsilon)^{-4} - 8\right)\rho^2\right] \times \left(\frac{2e^{-(1/12.5)n}}{1+e^{-(1/12.5)n}} - 1\right) - 2^{n+2}\varepsilon\rho^n \sin(n\theta) + 2 - 8\rho^2. \tag{6}$$

Correspondingly, the static flow resistivity of the petal-shaped hole is

$$\sigma = \frac{\Delta P}{tU} = \frac{32\mu}{d^2}\left[\frac{1}{(1-2\varepsilon)^4} + \left(1 - \frac{1}{(1-2\varepsilon)^4}\right)\frac{2e^{-(1/12.5)n}}{1+e^{-(1/12.5)n}}\right], \tag{7}$$

where ΔP is the pressure drop between the two ends of the hole, t is the thickness of hole, U is the average velocity of air inside the hole, $32\mu/d^2$ is the static flow resistivity of circular tube, and the items in parentheses represent the effect of petal-shaped section on static flow resistivity.

To connect air flow properties with acoustic properties, the drag forces of air inside the petal-shaped hole are calculated using the equivalent fluid model. The equivalent fluid model describes the perforated panel by two frequency-dependent physical parameters, i.e., effective density $\rho_{eq}(\omega)$ and dynamic bulk modulus $K_{eq}(\omega)$. By adopting the model of Pride *et al.* for effective density,[10] the specific acoustic impedance Z' of the MPP can be obtained as

$$Z' = j\omega\rho_0 t \times \left\{\frac{\nu}{j\omega q_0}\left[1 - b + b\sqrt{\left(1 + \left(\frac{2\alpha_\infty q_0}{b\Lambda}\right)^2 \frac{j\omega}{\nu}\right)}\right] + \alpha_\infty\right\}, \tag{8}$$

where the kinematic viscosity $\nu = \mu/\rho_0$, the viscous permeability $q_0 = \mu/\sigma$, α_∞ is the tortuosity (here $\alpha_\infty = 1$ since the petal-shaped hole is straight), and the viscous characteristic length $\Lambda = \sqrt{8\mu\alpha_\infty/\sigma}$. The parameter of tortuosity ratio $b = \alpha_\infty/[4(\alpha_0 - \alpha_\infty)]$, where α_0 is the static tortuosity, a physical parameter to evaluate the complexity of the path for air to flow through the perforation. Note that the tortuosity ratio b is strongly related to the cross-sectional shape of the hole. For circular perforations, $b = 3/4$. In this case, Eq. (8) together with the following Eq. (10) covers the classical Maa's theory for MPPs with circular perforations. In a viscous fluid flow, let $u_m(M)$ denote its microscopic velocity at position M. Its macroscopic velocity $u(M_0)$ is obtained by averaging $u_m(M)$ over a representative elementary volume V around M_0, that is, $u(M_0) = \langle u_m(M)\rangle_v$. The static tortuosity is defined as

$$\alpha_0 = \langle u_m^2(M)\rangle_v / u^2(M_0). \tag{9}$$

It is seen from Eq. (9) that the more uneven the velocity distribution, the larger the static tortuosity. With the velocity distribution of fluid flowing across a petal-shaped channel given by Eq. (6), the static tortuosity is determined from Eq. (9) so as to calculate the tortuosity ratio b. Finally, these results are submitted into Eq. (8) to calculate the specific acoustic impedance of the MPP having petal-shaped micro-perforations, as given later in Eq. (10).

The predicted tortuosity ratios of petal-shaped holes with different morphological parameters (i.e., wave number and relative roughness) are listed in Table I. These tortuosity ratios are taken to the third decimal point to ensure sufficient accuracy, so that one can adopt the results of Table I to determine the sound absorption coefficient of a MPP with petal-shaped holes. Figure 2 displays how the tortuosity ratio changes with the wave number and relative roughness of the petal-shaped perforation. When increasing the relative roughness or wave number, the boundary layer area increases, which implies a larger static tortuosity, thus the tortuosity ratio is reduced. That is, increasing either the relative roughness or wave number enlarges the cross-sectional perimeter of the micro-perforation, which affects the velocity distribution inside the cross-section, causing the tortuosity ratio to decrease. In turn, the tortuosity ratio affects the acoustic impedance of the MPP.

TABLE I. Tortuosity ratios of petal-shaped holes with different morphological parameters.

ε	0	0.01	0.02	0.03	0.04	0.05	0.06	0.07	0.08	0.09	0.10
$n=1$	0.75	0.743	0.733	0.719	0.702	0.681	0.656	0.629	0.599	0.566	0.531
$n=2$	0.75	0.739	0.724	0.705	0.682	0.656	0.626	0.592	0.556	0.516	0.474
$n=3$	0.75	0.734	0.714	0.690	0.662	0.630	0.594	0.555	0.513	0.468	0.421
$n=4$	0.75	0.730	0.704	0.675	0.641	0.604	0.564	0.520	0.473	0.425	0.375
$n=5$	0.75	0.724	0.694	0.660	0.622	0.580	0.535	0.488	0.439	0.388	0.337
$n=6$	0.75	0.720	0.685	0.646	0.604	0.559	0.510	0.459	0.408	0.356	0.305
$n=7$	0.75	0.715	0.676	0.633	0.587	0.537	0.486	0.434	0.381	0.329	0.278
$n=8$	0.75	0.711	0.668	0.620	0.570	0.518	0.465	0.411	0.358	0.306	0.256
$n=9$	0.75	0.707	0.659	0.609	0.555	0.501	0.445	0.391	0.338	0.287	0.238
$n=10$	0.75	0.703	0.651	0.597	0.541	0.484	0.428	0.373	0.321	0.271	0.224
$n=11$	0.75	0.699	0.644	0.587	0.528	0.470	0.412	0.358	0.306	0.257	0.212
$n=12$	0.75	0.695	0.637	0.577	0.516	0.456	0.398	0.344	0.293	0.246	0.202

https://doi.org/10.1121/10.0001462

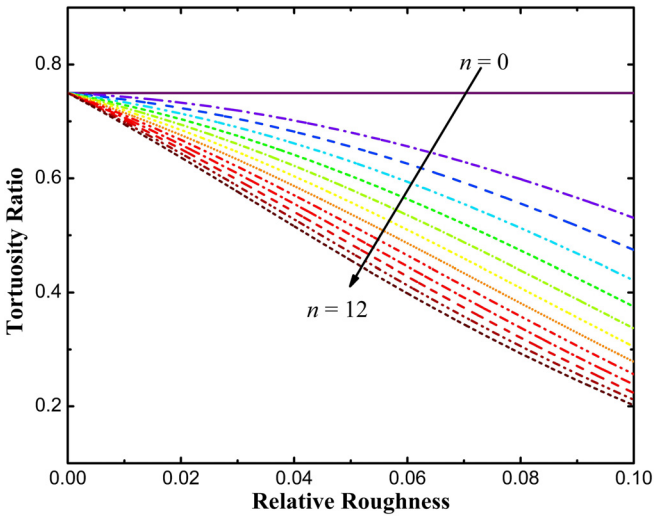

FIG. 2. (Color online) Influence of wave number and relative roughness on the tortuosity ratio of the MPP with petal-shaped micro-perforations.

Following the classical Maa's theory,[2,3] with the end effect of micro-perforation accounted for, the acoustic impedance of MPP z' can be calculated as

$$z' = r' + j\omega m' = \frac{Z'}{\phi\rho_0 c} + \frac{4\sqrt{2}\mu k}{\rho_0 \phi c d} + \frac{0.85 j\omega d}{\phi c}, \tag{10}$$

where (r', m') are the relative acoustic resistance and relative acoustic mass, respectively. It should be pointed out that, in Eq. (10), the end correction obtained by Maa[2,3] for circular perforations is adopted for the correction only accounts for a small proportion of the whole acoustic impedance (in fact, less than 10% for both the real part and imaginary part of acoustic impedance for all the cases considered in the present study). (If needed, however, one can resort to computation process detailed in Ingard[11] if more precise expression of the end correction is required.) Finally, with (r, m) in Eq. (2) replaced by (r', m'), the sound absorption coefficient of the MPP with petal-shaped perforations is determined.

To validate the present sound absorption model for MPPs with petal-shaped perforations, finite element simulations within the Thermoviscous Acoustics Module of COMSOL Multiphysics are performed. With the viscosity and thermal conduction of air taken into consideration, the equations governing the air flow are

$$\begin{aligned} i\omega\rho_0\mathbf{u} &= \nabla\cdot\left\{-p\mathbf{I} + \mu\left[\nabla\mathbf{u} + (\nabla\mathbf{u})^{\mathrm{T}} - \left(\frac{2}{3}\mu - \mu_B\right)(\nabla\cdot\mathbf{u})\mathbf{I}\right]\right\} \\ i\omega\rho + \rho_0\nabla\cdot\mathbf{u} &= 0 \\ i\omega T\rho_0 C_p - i\omega\alpha_p T_0 p &= \nabla\cdot(\kappa\nabla T), \end{aligned} \tag{11}$$

where $\mathbf{u}$ is the velocity of air particle; p, ρ and T represent the sound pressure, excess density, and excess temperature of air, respectively; $(\,)^{\mathrm{T}}$ is the matrix transpose operator; μ_B is the bulk viscosity of air; C_p, κ, and α_p are the specific heat at constant pressure, thermal conductivity, and thermal expansion coefficient of air; and T_0 is the ambient temperature.

As the distance between two adjacent holes on a MPP is typically large relative to hole size, the coupling effect between the holes is neglected. In other words, every hole in the MPP can be independently considered using a periodic unit. Because the fluid–solid coupling effect is assumed negligible in the current study, only air regions are created, as shown in Fig. 3(a). The perfectly matched layer is used to simulate the infinite boundary conditions by absorbing all the sound waves propagating into it. On the interfaces between the air and the MPP solid structure, no-slip and isothermal boundaries are adopted:

$$\begin{aligned} \mathbf{u} &= 0, \\ T &= 0. \end{aligned} \tag{12}$$

During the process of numerical simulation, the relative surface impendence of the MPP is calculated by

$$z_s = \frac{\langle p_\perp\rangle_s}{\langle v_\perp\rangle_s}\cdot\frac{1}{\rho_0 c}, \tag{13}$$

where $p_\perp$ and $v_\perp$ are the sound pressure and air particle velocity along the perpendicular direction to the MPP surface, and $\langle\rangle_s$ refers to the average over the MPP top surface. By extracting the relative acoustic resistance and relative acoustic mass from Eq. (13) and then substituting them into Eq. (2), eventually, the numerically simulated sound absorption coefficient is obtained.

Figure 3 compares the theoretical model predictions with FE simulation results of sound absorption coefficient for both circular and petal-shaped perforations. With $d = 1$ mm, $t = 6$ mm, $D = 50$ mm, $\phi = 0.0625$, $\varepsilon = 0.1$, and $n = 8$, the low-frequency limit of parameter b is obtained as 0.25628. For both circular and petal-shaped micro-perforations, the theoretical predictions match well with the numerical results. Altering the cross-section shape of the micro-perforation is seen to greatly affect the sound absorption performance of the MPP. For the case considered in Fig. 3, the peak sound absorption coefficient of the MPP is increased by over 20% when the circular micro-perforations are replaced by petal-shaped ones while all other parameters of the MPP remain unchanged. Nonetheless, the resonant frequency at which the sound absorption coefficient peaks is almost unaffected. In comparison with the circular perforations, for the same perforation area, the petal-shaped perforations actually increase the contact area between the air and the solid in the perforation hole, which thus significantly enhance the sound energy consuming by the friction effect when the viscous air vibrates in and out the perforation hole. As a result, the petal-perforations exhibit a better sound absorption performance than the circular ones, as shown in Fig. 3(b).

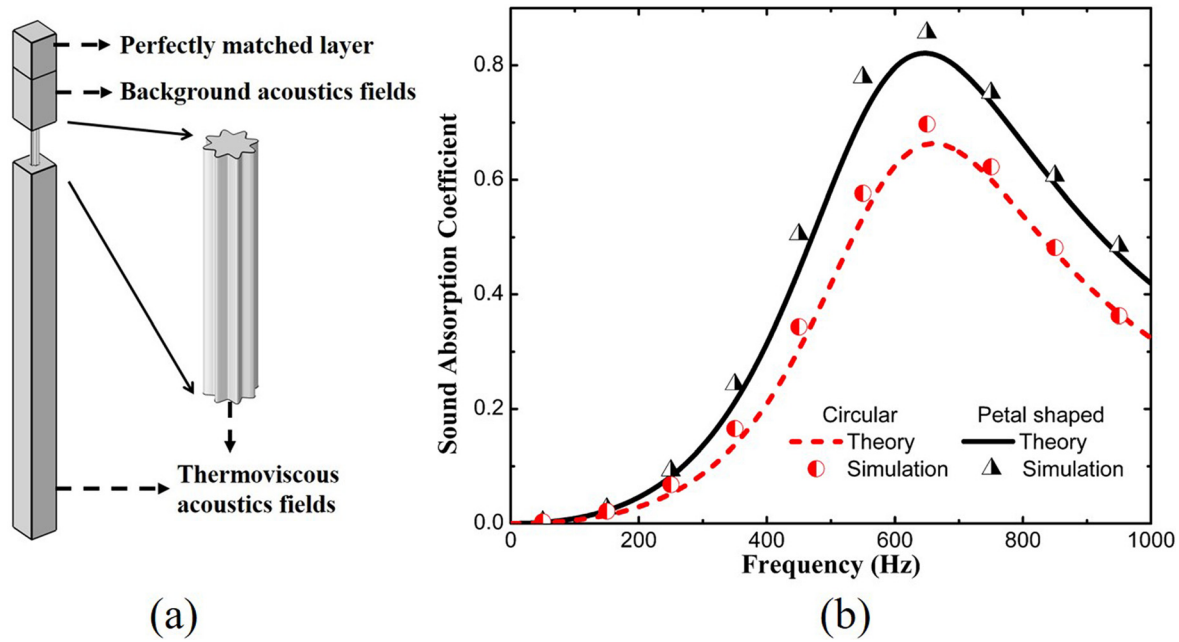

FIG. 3. (Color online) (a) Finite element model of one petal-shaped hole; (b) sound absorption coefficients of MPPs with circular and petal-shaped perforations: comparison between theoretical predictions and FE simulation results, with $d = 1$ mm, $t = 6$ mm, $D = 50$ mm, $\phi = 0.0625$, $\varepsilon = 0.1$, $b = 0.256$, and $n = 8$.

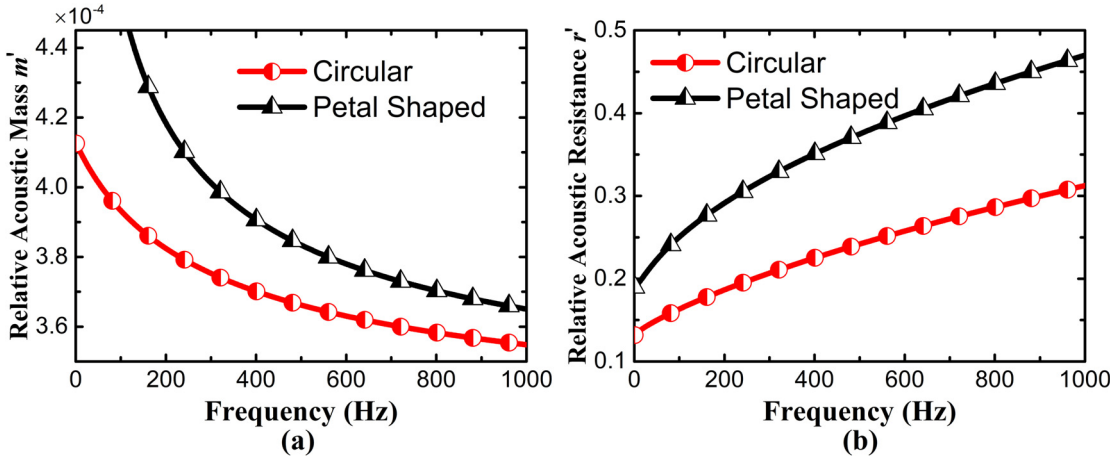

FIG. 4. (Color online) (a) Relative acoustic mass and (b) relative acoustic resistance of MPPs with circular and petal-shaped holes ($d = 1$ mm, $t = 6$ mm, $D = 50$ mm, $\phi = 0.0625$, $\varepsilon = 0.1$, and $n = 8$).

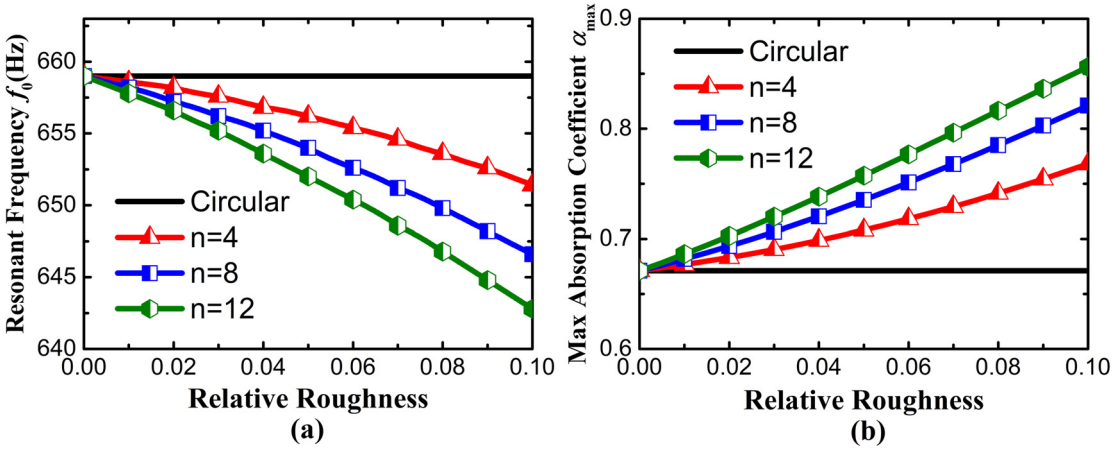

FIG. 5. (Color online) (a) Resonant frequency and (b) maximal (peak) absorption coefficient of MPPs with circular and petal-shaped holes ($d = 1$ mm, $t = 6$ mm, $D = 50$ mm, $\phi = 0.0625$).

https://doi.org/10.1121/10.0001462

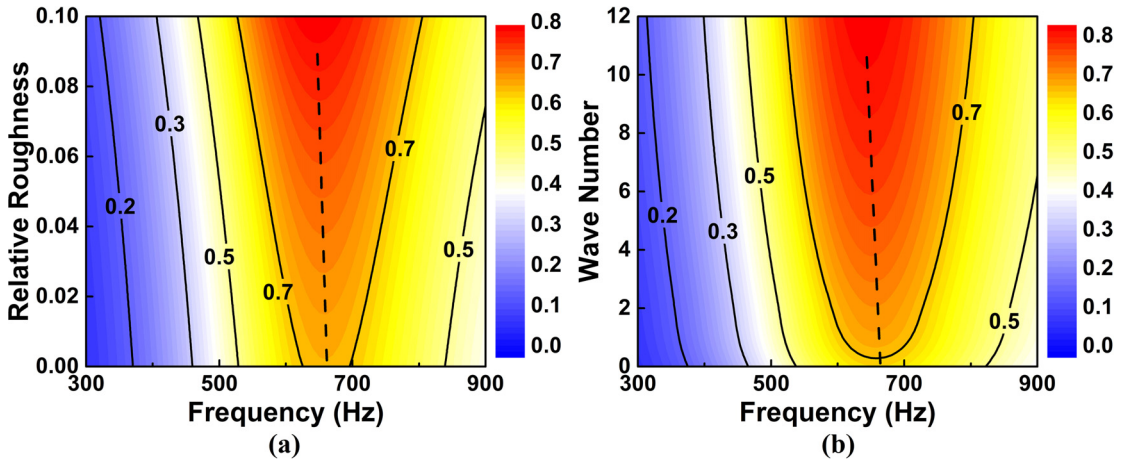

FIG. 6. (Color online) Influence of morphological parameters on sound absorption coefficient of the MPP with petal-shaped micro-perforations ($d = 1$ mm, $t = 6$ mm, $D = 50$ mm, $\phi = 0.0625$): (a) relative roughness ($n = 8$); (b) wave number ($\varepsilon = 0.1$). Dashed line: location of resonant frequency.

Figure 4 plots the theoretically predicted relative acoustic mass and relative acoustic resistance of the MPP as functions of frequency for both circular and petal-shaped micro-perforations. Relevant parameters adopted are identical to those in Fig. 3. Compared to circular micro-perforations, the contact area between air and wall in petal-shaped micro-perforations is larger, thus a thicker viscous boundary layer. As a result, both the relative acoustic mass and the relative acoustic resistance of the MPP with petal-shaped micro-perforations are enlarged. This also explains why a MPP with petal-shaped micro-perforations has superior absorption performance [Fig. 3(b)] for it largely depends on the viscous effect to dissipate sound energy. As the frequency is increased, air particles in the micro-perforations oscillate more severely, implying that the inertia effect protecting the velocity from changing (relative acoustic mass) decreases. In contrast, increasing the frequency enables more intense friction between the air and solid wall and hence the acoustic resistance is enlarged.

Next, the resonant frequency is calculated using the relative acoustic mass and acoustic resistance. As shown in Fig. 5(a), the resonant frequency of the MPP is slightly reduced (within 20 Hz) as the perforation shape is changed from circular to petal. Upon increasing either the relative roughness or the wave number, the image part of the acoustic impedance Z' increases as a result of the increased tortuosity ratio b (Fig. 2), thus causing the relative acoustic mass m' to increase as well. Consequently, the resonant frequency decreases with increasing relative roughness or wave number as shown in Fig. 5(a). According to Eq. (3), the sound absorption coefficient peaks when the relative acoustic resistance equals to unity. Depending upon the relative roughness or wave number, the petal-shaped hole can be tailored to have a significantly larger perimeter than the circular hole, enabling therefore a larger viscous boundary area and more viscous dissipation. As a result, the MPP with petal-shaped holes possesses a larger maximal (peak) absorption coefficient than the MPP with circular holes. Further, as is shown in Fig. 5(b), this peak absorption coefficient increases with increasing relative roughness or wave number, or both.

To better illustrate how the key morphological parameters of petal-shaped perforations on sound absorption, Fig. 6 displays two contour maps, one for relative roughness and another for wave number. The sound absorption coefficient is depicted using different colors, ranging from blue to red as it is increased in magnitude. The dashed line is introduced to show how the resonant frequency varies with varying relative roughness or wave number. As shown in Fig. 6, when either the relative roughness or wave number is increased, the resonant frequency at which the absorption coefficient is maximized decreases a little while the absorption coefficient increases, which is in accordance with the variation trends shown in Fig. 5.

In conclusion, the sound absorption theory for MPP with petal-shaped perforations has been successfully established to account for the effect of petal-shaped cross section. By numerical simulations utilizing the finite elements method, the sound absorption theory is validated and good agreement is achieved. Compared to circular perforation, the petal-shaped perforation decreases the resonant frequency and increases the max absorption coefficient of MPP. This work proposes a general MPP theory that not only contains the classical Maa's theory for circular MPP, but also accounts for the MPP with petal-shaped perforations.

ACKNOWLEDGMENTS

This work was supported by NSFC (11761131003, U1737107, and 11772248), DFG (ZH15/32-1), and the Fundamental Research Funds for the Central Universities.

[1]J. Liu, X. Hua, and D. W. Herrin, "Estimation of effective parameters for microperforated panel absorbers and applications," Appl. Acoust. **75**, 86–93 (2014).
[2]D. Y. Maa, "Theory and design of microperforated panel sound-absorbing constructions," Sci. Sin. **18**(1), 55–71 (1975).
[3]D. Y. Maa, "Potential of microperforated panel absorber," J. Acoust. Soc. Am. **104**(5), 2861–2866 (1998).

[4]C. Yang, "On the realization of acoustic attenuation using a microperforated panel alone," J. Acoust. Soc. Am. **143**(2), 1102–1105 (2018).
[5]C. Yang, "Acoustic attenuation of a curved duct containing a curved axial microperforated panel," J. Acoust. Soc. Am. **145**(1), 501–511 (2019).
[6]Z. Xu, X. Peng, X. Liu, F. X. Xin, and T. J. Lu, "Modified theory of a microperforated panel with roughened perforations," Europhys. Lett. **125**(3), 34004 (2019).
[7]S. Ren, X. Liu, J. Gong, Y. Tang, F. X. Xin, L. Huang, and T. J. Lu, "Tunable acoustic absorbers with periodical micro-perforations having varying hole shapes," Europhys. Lett. **120**(4), 44001 (2017).
[8]Y. Guo, S. Allam, and M. Åbom, "Micro-perforated plate for vehicle applications," in *Proceedings of the 2008 Congress and Exposition of Noise Control Engineering, Inter-Noise 2008*, Shanghai, China (October 26–29, 2008).
[9]Z. Xu, S. Song, F. X. Xin, and T. J. Lu, "Mathematical modeling of Stokes flow in petal shaped pipes," Phys. Fluids **31**(1), 013602 (2019).
[10]S. R. Pride, F. D. Morgan, and A. F. Gangi, "Drag forces of porous-medium acoustics," Phys. Rev. B **47**(9), 4964 (1993).
[11]U. Ingard, "On the theory and design of acoustic resonators," J. Acoust. Soc. Am. **25**(6), 1037–1061 (1953).